

Sensitivities to secret neutrino interaction at FASER ν

Majid Bahraminasr,¹ Pouya Bakhti,^{1,2} and Meshkat Rajaei^{1,2}

¹*Institute for research in fundamental sciences (IPM), PO Box 19395-5531, Tehran, Iran*

²*Jeonbuk National University, Jeonrabuk-do 54896, South Korea*

Abstract

We study the impact of the coupling of neutrinos with a new light neutral gauge boson, Z' , with a mass of less than 500 MeV in FASER ν experiment. Scenarios in which a light gauge boson is coupled to neutrinos are motivated within numerous contexts which are designed to explain various anomalies in particle physics and cosmology. This interaction leads to a new decay mode for charged mesons to a light lepton plus neutrino and Z' , ($\pi^+(K^+) \rightarrow e^+\nu Z'$) followed by the subsequent decay of Z' into the pair of neutrino and anti-neutrino, ($Z' \rightarrow \nu\bar{\nu}$). FASER ν , the Forward Search Experiment at the LHC, has the potential to detect collider neutrinos for the first time. In particular, the FASER ν emulsion detector will provide the opportunity to detect τ -neutrinos and to measure their energies. Using this ability of FASER ν emulsion detector, we investigate the potential of FASER ν experiment and the proposed upgraded version of this experiment, FASER2 ν , to constrain the coupling of a neutrino with the light gauge boson.

I. INTRODUCTION

Although particle colliders produce neutrinos of all flavors copiously, collider neutrinos have not yet been detected for two main reasons. First, neutrinos interact very weakly and second, collider detectors miss the enormous flux of high-energy neutrinos streaming down the beam pipe and are blind to the regions along the beamline. FASER, the Forward Search Experiment at the Large Hadron Collider (LHC) is going to be located 480 m downstream of the ATLAS interaction point along the beam collision axis. FASER's location is ideal to cover this blind region. Having such an ideal location, FASER will provide sensitive searches for light and weakly interacting particles in Run 3 from 2022 to 2024. FASER's neutrino detection capability is briefly discussed in [1] and more detailed studies on the detector design are reported in [2].

FASER ν is a sub-detector that will be able to detect the collider neutrinos for the first time [3]. FASER ν will be located in front of FASER spectrometer at CERN [3]. Depending on the neutrino flavor, the mean energy of neutrinos interacting in FASER ν is between 600 GeV and 1 TeV with a significant number of neutrino events up to 3 TeV. FASER ν will detect the most energetic neutrinos from the known source. The other advantage of FASER ν is its emulsion detector that has the greatest precision to detect tau-neutrinos. Detecting a tau-neutrino requires that the neutrino beam has enough energy to produce a tau lepton ($E_{\nu_\tau} > 3.5$ GeV). On the other hand, tau leptons are short-lived and decay promptly. This makes their identification extremely hard. Having an integrated luminosity of 150 fb^{-1} , FASER ν will be a good apparatus to identify the tau-neutrinos and to study the new neutrinophilic interaction with tau-neutrino detection.

Being able to observe these interactions and reconstruct their energies, FASER ν will probe the production, propagation, and interactions of neutrinos at very high energies (TeV). Since FASER ν benefits from high-energy neutrinos producing from very high-energy mesons, it is interesting to investigate the possibility of interaction of neutrinos with new light particles using this experiment. FASER2 is a proposed upgraded version of the FASER experiment, with several hundred to thousand times larger data collection due to higher luminosity and spectrometer dimensions. It is also proposed to use a larger emulsion neutrino detector in front of the FASER2 tunnel.

In the present paper, we study the scenario in which neutrinos couple to a light gauge boson Z' with a mass smaller than ~ 500 MeV. Neutrinophilic new gauge interaction with a light gauge boson is motivated by so-called ν -DM models. As proposed in [4–6], they can help to solve small-scale structure problems that appear in the canonic collisionless cold dark matter paradigm. If the new gauge boson couples to matter fields, scattering experiments will be able to detect it. Besides, it can affect the neutrino oscillation in the matter. However, if Z' couples only to the neutrinos, it will not affect neutrino oscillation in the matter or elastic scattering of neutrinos off nuclei. Moreover, assuming that only neutrino couples to the new gauge boson, Z' decays only into neutrinos at tree level, appearing as missing energy in the experiments. Assuming the standard meson two-body decay ($M \rightarrow l\nu$), the decay rate is suppressed by m_l^2/m_M^2 . Assuming the three-body decay of the Meson ($M \rightarrow l\nu Z'$), the decay rate receives an enhancement of $m_M^2/m_{Z'}^2$, from longitudinal polarization; Thus, it

can provide us an opportunity to search for even small gauge coupling.

In this work, we study how decays of charged mesons ($M \rightarrow l\nu Z'$) can provide us information about neutrinos interacting with new light particles. We will investigate the sensitivity of leptonic decay of charged mesons to the interaction of neutrinos with Z' . In our scenario, a new gauge boson with a mass of less than 500 MeV can be produced via $M \rightarrow l\nu Z'$ and subsequently Z' decays into a pair of a neutrino and an anti-neutrino before reaching the near detector. The produced neutrinos can be detected, providing us with information on the intermediate Z' .

Several models for neutrino interaction with the new light gauge boson have been proposed in the literature. One possible underlying model that can lead to this interaction is proposed in reference [7, 8], introducing a new fermion of a mass of the order of GeV that is charged under an extra U(1) gauge symmetry. This new fermion is mixed with neutrino and the active neutrinos will obtain interactions of this form.

This interaction can lead to a new mode of meson decay, $M \rightarrow l\nu Z'$, and subsequently, Z' decays to neutrino anti-neutrino pair. Charged meson decays and short-baseline accelerator-based neutrino experiments are sensitive probes of this neutrinophilic interaction of light new particles. The most stringent current constraint on the coupling comes from kaon decay rare event measurement at NA62 in the range of MeV to a few ten MeV [9, 10]. Furthermore, the near detector of DUNE [11], will constrain the scenario more stringently, due to a large number of statistics and tau-neutrino detection with low background [12]. FASER ν has the advantage of producing neutrinos from massive mesons such as charm mesons and therefore, it can help to constrain the coupling in larger mass range of $m_{Z'}$. Moreover, it benefits from large efficiency of tau neutrinos as well as large values of neutrino energy, so it has a great potential to determine g_{ee} , $g_{e\tau}$, $g_{e\mu}$ and $g_{\mu\tau}$ separately by studying the electron neutrino and tau neutrino signals. In this paper we study this possibility to constrain g_{ee} , $g_{e\tau}$, $g_{e\mu}$ and $g_{\mu\tau}$ using FASER ν and FASER2 ν data.

The present paper is organized as follows. In Sec. II, we present a short review of the new Lagrangian and the decay rates. In Sec. III, the details of the FASER ν experiment and our simulation are discussed. In Sec. IV, we present our results. Sec. V is dedicated to the summary and discussion.

II. LEPTOPHILIC GAUGE INTERACTION, MESON DECAY, AND NEUTRINO

The interaction of the neutrino of flavor α with the new vector boson Z' is given by

$$\sum_{\alpha,\beta} g_{\alpha\beta} Z'_\mu \bar{\nu}_\alpha \gamma^\mu \nu_\beta \quad (1)$$

where $g_{\alpha\beta}$ is the the couplings between the new light boson Z' and neutrinos of flavor α and β . There are various underlying models leading to such an interaction. Notice that this secret interaction of neutrino with new gauge boson suffers from non-invariance under $SU(2)_L$. Gauging anomaly free combination of lepton flavors and baryon number can lead to this interaction. Gauging various combinations of lepton flavors and baryon number

$a_e L_e + a_\mu L_\mu + a_\tau L_\tau + bB$ can lead to such an interaction, where a_e, a_μ, a_τ and b are real numbers satisfying the anomaly cancellation condition. There are strong bounds on the coupling of the electron to Z' from various observations [13]. Current constraints on their parameter spaces and the sensitivity of DONuT and as well as the future emulsion detector experiments FASER ν , LHC and SHiP on four scenarios of anomaly free U(1) gauge groups corresponding to the $B - L$, $B - L_\mu - 2L_\tau$, $B - L_e - 2L_\tau$ and $B - 3L_\tau$ are presented in [13]. The strongest direct constraints in parts of the parameter space of the $B - L_e - 2L_\tau$ and $B - 3L_\tau$ models are imposed by the DONuT experiment. Since there are strong bounds on the coupling of the electron to Z' , we will not focus on this class of models.

Moreover, as it is discussed in ref. [7], another possibility is introducing a new Dirac fermion which is charged under the new U(1) gauge symmetry and can mix with the active neutrinos. Let us briefly review this scenario. The new fermion Ψ is assumed to be charged under the new U(1) and can mix with ν_α . Let us denote the gauge coupling by g_Ψ , the gauge interaction term can be written as $g_\Psi Z'_\mu \bar{\Psi} \gamma^\mu \Psi$. The active neutrinos of flavor ν_α can be written as a linear combination of mass eigenstates ν_i as $\nu_\alpha = \sum_{i=1}^4 U_{\alpha i} \nu_i$, where ν_4 is the heavier state giving the main contribution to Ψ . We assume ν_4 to be heavier than the charged meson M^+ , therefore, in the decay $M^+ \rightarrow l_\alpha^+ \nu + X$, where X could be any state, the coherent ν state is not exactly equal to ν_α and is a linear combination of ν_1, ν_2 and ν_3 which cannot be perpendicular to Ψ . Integrating out the heavy fourth state, the light active neutrinos receive a coupling of the form $g_{\alpha\beta} Z'_\mu \bar{\nu}_\alpha \gamma^\mu \nu_\beta$ in which $g_{\alpha\beta} = g_\Psi |U_{\Psi 4}|^2 U_{\alpha 4} U_{\beta 4}^* \simeq g_\Psi U_{\alpha 4} U_{\beta 4}^*$. As a result, three-body decays $M \rightarrow l_\alpha \nu_\beta Z'$ can take place with a rate proportional to $|g_{\alpha\beta}|^2$. Z' will subsequently decay into $\bar{\nu}_\alpha \nu_\beta$ again with a rate proportional to $|g_{\alpha\beta}|^2$. However, if ν_4 is lighter than the parent charged lepton, we cannot integrate it out and the picture will be different and this is not the case we are interested in this work. One method to mix Ψ with ν_α is to introduce a new Higgs doublet H' charged under the new U(1) such that its vacuum expectation value induces a mixing between Ψ and ν_α via a Yukawa coupling of the form $\bar{L}_\alpha H'^T c \Psi$ [14]. As discussed in this reference, in this scenario, Ψ cannot be lighter than a few MeV, otherwise, it contributes as an extra relativistic degree of freedom in the early Universe. On the other hand, it cannot be heavier than a few GeV to maintain the perturbative region and to satisfy the unitarity bounds. In the other model described in detail in [8] a neutral Dirac N and a new scalar singlet S charged under U(1) are introduced with interaction terms similar to that in the inverse seesaw mechanism: $Y_\alpha \bar{N}_R H'^T c L_\alpha + \lambda_L S \bar{\Psi}_R N_L$. and $U_{\alpha 4}$ is given by $Y_\alpha \langle H \rangle \lambda_L \langle S \rangle / (m_N m_\Psi)$. In this class of models, only neutrinos couple to Z' at tree level. Thus, they escape from the bounds on the coupling of the corresponding charged leptons to Z' . The bounds on the deviation of the PMNS mixing matrix from the unitarity can be translated into the bounds on $g_{\alpha\beta}$ [14]. For gauge coupling in the perturbative range, $g_\Psi \lesssim 4$, the bound from unitarity which is $|U_{e4}|^2 < 2.5 \times 10^{-3}$ [15] can be translated as $g_{ee} \lesssim 10^{-2}$. Notice that in this case, we are not introducing a new source of lepton flavor violating (LFV) so no strong bound comes from $\mu \rightarrow e\gamma$ and from similar LFV processes. The unitarity bound on $|U_{e4} U_{\tau 4}^*|$ is 3.7×10^{-3} [15] can lead to $g_{e\tau} \lesssim 10^{-2}$. The LFV process $\tau \rightarrow e\gamma$ does not yield a strong bound since it is GIM suppressed [14].

Let us now compute the flux of neutrinos from meson decay as well as from subsequent Z' decay. The new interaction leads to a new decay mode of meson decay to electron, neutrino

and Z' , with the decay rate of [10]

$$\Gamma(M \rightarrow l_\alpha \nu Z') = \frac{1}{64\pi^3 m_M} \int_{E_l^{min}}^{E_l^{max}} \int_{E_\nu^{min}}^{E_\nu^{max}} dE_l dE_\nu \sum_{spins} |\mathcal{M}|^2. \quad (2)$$

Neglecting the neutrino and lepton masses, the amplitude is

$$\sum_{spins} |\mathcal{M}|^2 = \left(\sum_{\beta} g_{\alpha\beta}^2 \right) G_F^2 f_M^2 V_{qq'}^2 (m_M^2 + m_{Z'}^2 - 2m_M E_{Z'}) \quad (3)$$

$$+ \frac{(m_M^2 - m_{Z'}^2 - 2m_M E_l)(m_M^2 - m_{Z'}^2 - 2m_M E_\nu)}{m_{Z'}^2}, \quad (4)$$

where G_F is the Fermi constant, $V_{qq'}$ and f_M are the relevant CKM mixing element and meson decay constant, respectively. In the case of m_e , integration limits are given by

$$E_e^{min} = m_e, \quad E_e^{max} = \frac{m_M^2 - m_{Z'}^2}{2m_M},$$

$$E_\nu^{min} = \frac{m_M^2 - m_{Z'}^2 - 2m_M E_e}{2m_M}, \quad E_\nu^{max} = \frac{m_M^2 - m_{Z'}^2 - 2m_M E_e}{2(m_M - 2E_e)}.$$

Notice that the above formulas are valid if we can neglect the lepton mass. In this case the decay rate can be calculated analytically. In the case of meson decay to muon ($M \rightarrow \mu \nu Z'$) and tau ($M \rightarrow \tau \nu Z'$), we calculate the meson decay rate numerically.

The number of neutrinos coming from Z' particles decaying before reaching the detector is given by

$$N = N_0 (1 - e^{-\Gamma L/\gamma}) \quad (5)$$

where N_0 is the number of produced Z' , L is the distance between the production point of Z' and the detector and $\gamma = E_{Z'}/m_{Z'}$ is the boost factor. As it can be seen from equation 5, if $\Gamma L/\gamma \gg 1$ almost all of the Z' particles decay before reaching the detector.

The estimated number of neutrinos coming from different meson decays passing through FASER ν detector is given in ref [2], assuming an integrated luminosity of 150 fb^{-1} for Run 3 at the 14TeV LHC. Considering the spectrum of neutrinos coming from pion, kaon and charm meson decay, we can reconstruct the spectrum of the initial meson. In the rest frame of the meson, the total spectrum of the neutrino produced from both meson and Z' decay is given by

$$\left(\frac{dN_\nu}{dE_\nu} \right)_{r.o.M} = \left(\frac{dN_\nu}{dE_\nu} \right)_{r.o.M}^{Z' \text{ decay}} + \frac{N_0}{\Gamma(M \rightarrow l\nu Z')} \frac{d\Gamma(M \rightarrow l\nu Z')}{dE_\nu} \quad (6)$$

where N_0 is the total number of the neutrinos produced from meson decay. $\Gamma(M \rightarrow e\nu Z')$ and $\frac{d\Gamma(M \rightarrow e\nu Z')}{dE_\nu}$ is determined from Eq. 2. The spectrum of neutrinos produced from Z' decay is determined with integration over the Z' spectrum in rest frame of meson multiplied by neutrino spectrum for a specific energy of Z' as follows

$$\left(\frac{dN_\nu}{dE_\nu} \right)_{r.M}^{Z' \text{ decay}} = \sum_i \int_{E_{Z'}^{min}}^{E_{Z'}^{max}} dE_{Z'} \frac{dN_{Z'}}{dE_{Z'}} \Big|_i \left(\frac{dN_\nu}{dE_\nu} \right)_{r.M} \Big|_i \quad (7)$$

where $E_{Z'}^{min} = E_\nu + m_{Z'}^2/(4E_\nu)$, $E_{Z'}^{max} = (m_M^2 + m_{Z'}^2)/(2m_M)$ and i refers to Z' different polarizations. The neutrino energy at the rest frame of Z' is given by $m_{Z'}/2$, and neutrino spectrum for a specific energy of Z' is calculated with boost of Z' . The neutrino spectrum in the lab frame is given by

$$\phi(E_\nu) = \frac{1}{4\pi L^2} \int_{E_M^{min}}^{E_M^{max}} dE_M P_M(E_M) \left(\frac{dN_\nu}{dE_\nu}\right)_{lab} \frac{d\Omega_{r.M}}{d\Omega_{lab}}, \quad (8)$$

where $P_M(E_M)$ is the differential meson spectrum in the lab frame and $(\frac{dN_\nu}{dE_\nu})_{lab}$ is the spectrum of the neutrino in the lab frame. $d\Omega_{r.M}/d\Omega_{lab} = (1 + v_M)/(4(1 - v_M)) \simeq \gamma_M^2$ takes care of focusing of the beam in the direction of the detector. v_M is the meson velocity in the lab frame and $\gamma_M = (1 - v_M^2)^{-1/2}$. For details of the calculation see the Appendix of Ref. [12] and Ref. [10].

III. FASER ν EXPERIMENT AND LIGHT Z'

FASER experiment is a spectrometer tunnel with a length of 1.5 m and a radius of 10 cm, 480 m downstream to the ATLAS interaction point. This apparatus will be sensitive to new physics measurements such as dark photons and axion-like particles [3]. FASER ν is a proposal to detect collider neutrinos for the first time using an emulsion detector in front of FASER spectrometer [3]. FASER ν consists of 1.2 tons tungsten plates and 1000 layers of emulsion films. The neutrino beam consists of both neutrino and anti-neutrino, and they will be detected with charged-current deep inelastic scattering from nuclei. The flavor of neutrinos is determined with the charged lepton detection. Assuming standard model cross-section, the total number of 20000, 1300, and 20, respectively for muon, electron, and tau-neutrinos will be detected. The neutrino energy is in the range of a few 10 GeV to a few TeV with the peak of neutrino interaction between 600 GeV to 1 TeV. In this energy range, ν_τ cross-section is large and approximately equal to electron and muon neutrino cross-sections. The cross-section of deep inelastic scattering is approximately proportional to the neutrino energy. In Ref. [3] the cross-section is calculated by considering NNPDF3.1NNLO parton distribution function [16].

As it is well known, the identification of tau leptons is extremely difficult. Directly detecting tau-neutrino requires that the neutrino beam has enough energy to produce a tau particle. With a spatial resolution of a few ten nm, emulsion detectors are the most sensitive for detecting the short-lived particles such as tau-neutrinos. FASER ν energy resolution is 30% and the neutrino energy is determined from leptonic and hadronic energies. The backgrounds of electron neutrino CC interaction detection are the shower of the neutral pion to photon pair, and pion decay to photon and electron-positron pair. The other source of background is muon neutrino CC interaction. Backgrounds of tau-neutrino CC interaction are neutral current interaction and CC interaction of electron and muon neutrino when they are associated with charm production at the interaction vertex. There are also accidental backgrounds. These backgrounds at FASER ν will be much smaller than other emulsion detectors like OPERA, due to larger neutrino energy. Moreover, by combining FASER and

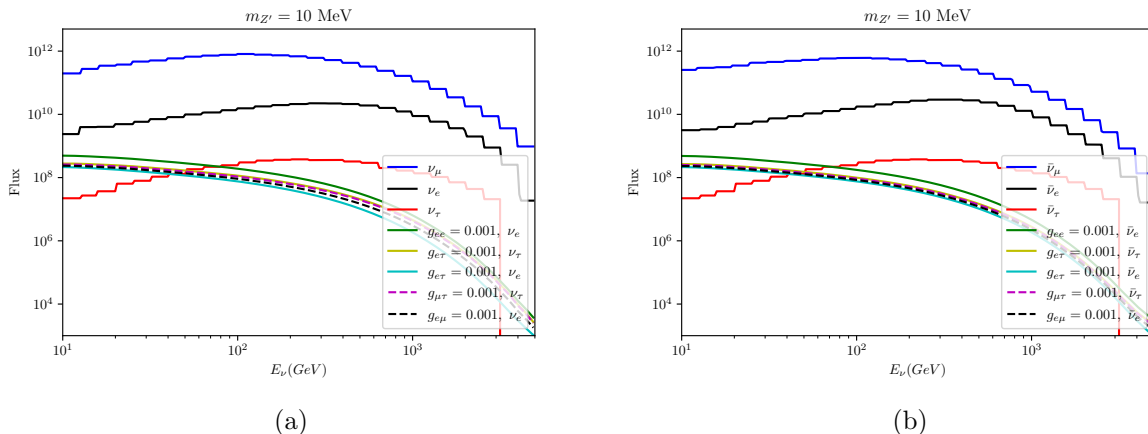


FIG. 1. The estimated number of neutrinos (left panel) and antineutrino (right panel) passing through the detector of FASER ν experiment for muon, electron, and tau neutrinos assuming an integrated luminosity of 150 fb^{-1} for the Run 3 at the 14 TeV LHC. The blue, black and the red curves are plotted for ν_μ ($\bar{\nu}_\mu$), ν_e ($\bar{\nu}_e$) and ν_τ ($\bar{\nu}_\tau$), respectively, in the left (right) panel assuming the standard model as the true model. To plot other curves, we have assumed $m_{Z'} = 10 \text{ MeV}$ and $g_{\alpha\beta}$ is set to 0.001.

FASER ν , we can distinguish between ν_μ and $\bar{\nu}_\mu$. Due to the long lifetime of a muon, the produced muon at FASER ν will pass through FASER spectrometer.

FASER2 is a proposed experiment similar to FASER, with twenty times larger luminosity and mass detector of 100 times larger than FASER [3]. It is also proposed to locate a larger emulsion neutrino detector in front of the FASER2. The mass of the detector is under discussion. Also in Ref. [3] a mass of 10 to 1000 tons is proposed while in Ref. [29] a mass of the order of ten tons is mentioned. In our analysis, we have considered the maximum possible future statistics for the detection of neutrinos at FASER2 which is approximately 100 and 1000 times larger data than FASER ν . All the details of the analysis of FASER2 ν are the same as FASER ν , except for the statistics. In the following, we will show that FASER ν has the potential to set a more stringent bound on the coupling for the mass range of $50 \text{ MeV} < m_{Z'} < 150 \text{ MeV}$. However, the upgraded version of FASER ν will constrain our scenario more stringently than the current bound in the range of $m_{Z'} < 2 \text{ keV}$ and $3 \text{ MeV} < m_{Z'} < 200 \text{ MeV}$.

IV. CONSTRAINTS

In this section, we discuss how the data from the FASER ν and FASER2 ν can be used to extract information on the coupling of neutrinos to the new gauge boson. The spectrum of produced neutrinos from different decay modes is presented in Ref. [3]. 2×10^{11} electron neutrinos, 6×10^{12} muon neutrinos, 4×10^9 tau-neutrinos and a comparable anti-neutrinos pass through the FASER ν detector. As mentioned in Ref. [3] tau-neutrinos are mainly

produced from D_s , strange charm meson (Fig.4 of Ref. [3]). To find the spectrum of D_s , we have taken the neutrino spectrum and assumed that all the produced neutrinos are coming from $D_s \rightarrow \tau\nu_\tau$. Noticing that the branching ratio of $D_s \rightarrow \tau\nu_\tau$ is $(5.6 \pm 0.4)\%$. As we will see in the following this decay channel is very important for constraining $g_{\alpha\beta}$, especially for $m_{Z'} > 50$ MeV.

Considering the new interaction, electron and/or tau-neutrinos can be produced from meson three-body decay, $M \rightarrow l\nu_\alpha Z'$, and subsequent Z' decay to neutrino-antineutrino pair. Pion and kaon leptonic decays are the dominant modes of neutrino production reaching to the FASER ν detector [3]. Moreover, we also consider the subdominant production channel $D_s \rightarrow l\nu_\alpha Z'$, because of the large mass of D_s , ($m_{D_s} = 1968.47 \pm 0.33\text{MeV}$). This large mass of strange charm meson is noticeable for large Z' mass since this can allow us to constrain Z' with larger mass range [$m_{Z'} > 50$ MeV]. However, there is also a contribution from D^+ and D^- decays. We have not taken this into account for simplicity. The spectrum of neutrinos produced from both meson three-body decay and Z' decay is given by Eq. 8. The main source of the background of electron and tau-neutrinos is the intrinsic background. Several experiments such as KLOE II [17], NA48 [18], NA62 [9], $K^+ \rightarrow e^+\nu\bar{\nu}$ [19], $K^+ \rightarrow \mu^+\nu\bar{\nu}$ [20] and E949 [21] have studied kaon decay with an unprecedented accuracy. For $1 \text{ keV} < m_{Z'} < 2 \text{ MeV}$ also the stringent bound comes from Big Bang Nucleosynthesis (BBN) which is several orders of magnitudes stronger than NA62 bound [27]. Below 1 keV, the most stringent bound is set by NA62. Moreover, the NA62 experiment [9, 10] provides the best measurement and finds the most stringent bound from 1 – 60 MeV. For $m_{Z'} > 60$ MeV, the strongest constraint comes from invisible decay of Z [23]. We consider pion, kaon and strange charm meson decay and find the constraint on the coupling of a neutrino with the light gauge boson for $1 \text{ KeV} < m_{Z'} < 500 \text{ MeV}$. Notice the constraints on the coupling from meson decay has a linear behavior for $m_{Z'} < 1 \text{ MeV}$, thus for $m_{Z'} < 1 \text{ KeV}$ the constrain is a linear extrapolation of the results. Fig. 1 indicates muon, electron and tau (anti-) neutrino fluxes for $m_{Z'} = 10 \text{ MeV}$, assuming standard model and non-zero value for $g_{\alpha\beta}$ equal to 0.001.

For statistical inference, we used the chi-squared method. Depending on the number of events in each bin, we used Gaussian or Poisson distribution function, for a large and small number of events, respectively. We have considered the number of events smaller than twenty events as a small number of events. Taking the Asimov data set, we have considered two cases, first the standard model as the true model, and second the new gauge interaction as the true model. We have used the pull method to account for the systematic uncertainties. We have considered the flux normalization uncertainty of 10%. Other important systematic uncertainties come from the shape of the flux of ν_e and ν_τ . This is very crucial since taking into account the uncertainties in the shape of the background may change the results significantly. Estimating the systematic uncertainties of the ν_e and ν_τ spectrum is beyond the scope of this work. During our analysis, we take the couplings to be non-zero one at a time. We assume FASER2 ν has 100 and 1000 times larger data collection than FASER ν . The 90% constraints on $g_{e\tau}$ are shown in Fig. 2. The current constraints from meson decay experiments PIENU [26], NA62 [9] are indicated by yellow and red curves, respectively. Moreover, the current constraint from Z decay [28] and the BBN constraint [27] are indicated by the black

dashed and red dashed curves. To plot this figure, we assume that $g_{e\tau}$ is non-zero and set the other couplings equal to zero. Considering 10 years of data taking for DUNE near detector (ND), 5 years in each mode, we have shown the constraint from DUNE ND data by the black curve. The potential of FASER ν to constrain $g_{e\tau}$ is indicated by the blue curve. We observe that for $50 \text{ MeV} < m_{Z'} < 100 \text{ MeV}$, FASER ν can constrain $g_{e\tau}$ more stringent than current constraints and DUNE ND. Moreover, as can be observed for the number of events 100 (blue dashed) and 1000 (green dashed) times larger than FASER ν , FASER2 ν can constrain $g_{e\tau}$ stronger than the current constraints for $m_{Z'} < 2 \text{ keV}$ and $3 \text{ MeV} < m_{Z'} < 300 \text{ MeV}$.

It is also interesting to study the case of non-zero g_{ee} . In this case, g_{ee} is constrained by detecting electron (anti-)neutrino while in the case of nonzero $g_{e\tau}$, the coupling is constrained from both electron and tau (anti-)neutrino detection. In Fig. 3 the constraints on g_{ee} are shown. We have assumed that $g_{ee} \neq 0$ while setting other coupling to zero. Although FASER ν cannot constrain the coupling more stringent than the current one, we observe that FASER2 ν with 100 and 1000 times larger than FASER ν data taking can improve the constraint on g_{ee} for $m_{Z'} < 2 \text{ keV}$ and $3 \text{ MeV} < m_{Z'} < 200 \text{ MeV}$.

In Fig. 4, we have indicated the upper bound on $g_{\mu\tau}$ vs. $m_{Z'}$ at 90% C.L., assuming only $g_{\mu\tau} \neq 0$. The current bound from $K \rightarrow \mu\nu\nu\nu$ [20] and FASER ν [1] are shown by the yellow and the blue curves, respectively. The black dashed line shows the current constraint from Z decay and the red dashed curve indicates the BBN constraint. As can be observed, for the mass range $10 \text{ MeV} < m_{Z'} < 300 \text{ MeV}$, FASER2 ν with 1000 times larger data than FASER ν , can set the most stringent bound on $g_{\mu\tau}$ (green dashed curve).

Fig. 5 shows $g_{e\mu}$ vs. $m_{Z'}$ at 90% C.L., assuming only $g_{e\mu} \neq 0$. Again we observe that FASER2 ν with 1000 times larger data than FASER ν , can improve the constraint slightly in this case, for $15 \text{ MeV} < m_{Z'} < 300 \text{ MeV}$.

Notice that in the case of $g_{e\tau}$, FASER ν , itself can set bound on $g_{e\tau}$ more stringently than the current constraints as well as DUNE constraint for $50 \text{ MeV} < m_{Z'} < 150 \text{ MeV}$ while in the case of g_{ee} and $g_{\mu\tau}$ it cannot. This is because FASER ν can detect τ neutrinos with high efficiency. Moreover, considering heavy mesons such as strange charm meson which are produced at the interaction point, and their subsequent three-body decay can produce Z' is important to set a constraint on the coupling of neutrino with heavier Z' masses ($50 \text{ MeV} < m_{Z'} < 500 \text{ MeV}$). Our results show that for data 100 and 1000 times larger than FASER ν data, FASER2 ν can improve the constraint on the g_{ee} and $g_{e\tau}$ coupling for $m_{Z'} < 2 \text{ keV}$ and $3 \text{ MeV} < m_{Z'} < 300 \text{ MeV}$. Also FASER2 ν with 1000 times larger than FASER ν data, can slightly improve the constraint on $g_{e\mu}$.

V. SUMMARY

We have studied the constraints from meson decay on the coupling of neutrinos to a light new vector boson with a mass smaller than 500 MeV, using FASER ν emulsion detector and its upgraded version, FASER2 ν . Z' can be produced via three-body decay of the charged mesons, along with a charged lepton and a neutrino and can subsequently decay into a neutrino-antineutrino pair before reaching the detector. The produced neutrinos can be detected at the emulsion detector of FASER ν .

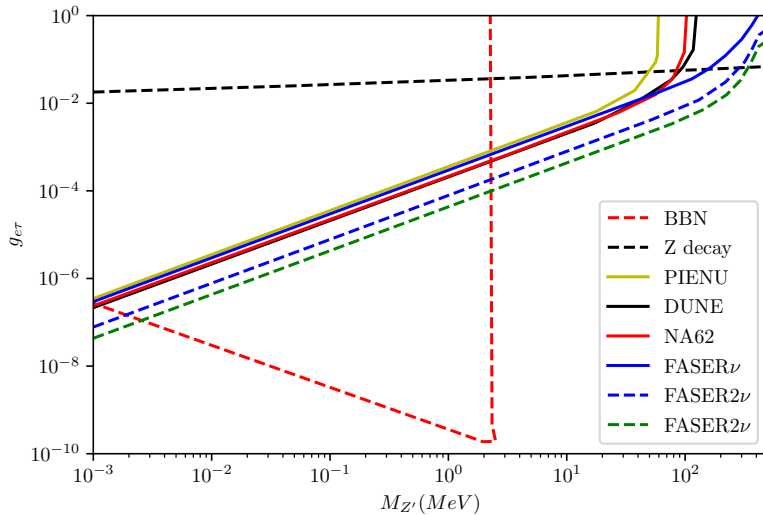


FIG. 2. The upper bound on $g_{e\tau}$ vs. $m_{Z'}$ at 90% C.L. The yellow, red and the blue curves shows the current bound from PIENU [26], NA62 [9] and FASER ν [1], respectively. The black curve corresponds to DUNE ND data assuming ten years of data taking. We have assumed detection efficiency of 2%. The blue dashed curve and the green dashed curve indicate the constraints from FASER2 ν corresponding to the assumed data of one hundred times and one thousand times larger than FASER ν , respectively. We have assumed detection efficiency of 80% for FASER ν . The black dashed line shows the current constraint from Z decay [28]. The red dashed curve shows the BBN constraint [27].

FASER ν , an inexpensive subdetector of FASER, will provide an opportunity to detect the first collider neutrinos; In particular, FASER ν will make it possible to study ν_e and ν_τ in detail at the highest energies yet explored. In this work, we have studied the potential of FASER ν and proposed an upgraded version of it, FASER2 ν , with higher statistics to constrain the secret neutrino gauge interaction. Considering secret neutrino gauge interaction, with $\sum_{\alpha,\beta} g_{\alpha\beta} Z'_\mu \bar{\nu}_\alpha \gamma^\mu \nu_\beta$ Lagrangian leads to new three-body charged meson decay mode, that charged lepton, neutrino and Z' will be produced and subsequently Z' decays to neutrino antineutrino pair. Our results are indicated in Fig. 2 to Fig. 5. As indicated in Fig. 2, using only FASER ν data, for $50 \text{ MeV} < m_{Z'} < 150 \text{ MeV}$, we can constrain $g_{e\tau}$ more strongly than the current constraints and future DUNE near detector constraint. However we observed that with 100 and 1000 times larger than FASER ν , FASER2 ν can improve the limit on $g_{e\tau}$ for $m_{Z'} < 2 \text{ keV}$ and $3 \text{ MeV} < m_{Z'} < 300 \text{ MeV}$.

Moreover, we showed that while FASER ν is not able to constrain g_{ee} better than DUNE and the current constraints, FASER2 ν with a data 100 and 1000 times larger than FASER ν data, can improve the constraint on the g_{ee} for the mass range of $m_{Z'} < 2 \text{ keV}$ and $3 \text{ MeV} < m_{Z'} < 300 \text{ MeV}$ (Fig. 3).

The results for $g_{\mu\tau}$ was indicated in Fig. 4. We observed that for the mass range $10 \text{ MeV} < m_{Z'} < 300 \text{ MeV}$, FASER2 ν with 1000 times larger data than FASER ν , can set the most

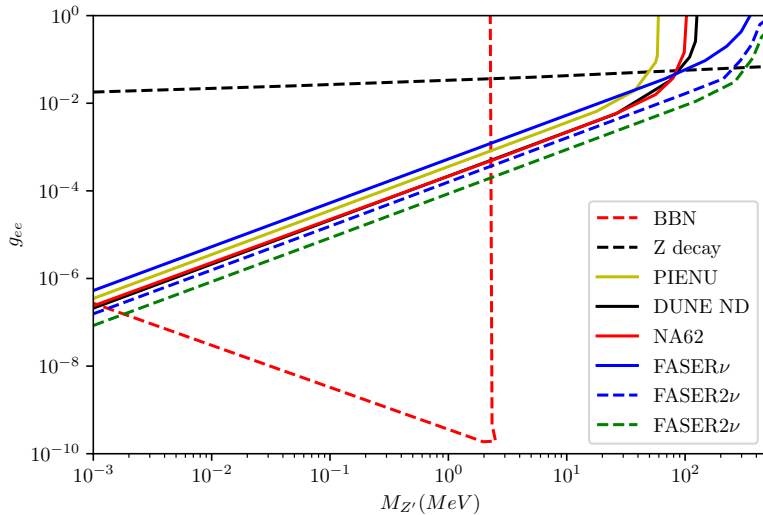


FIG. 3. The upper bound on g_{ee} vs. $m_{Z'}$ at 90% C.L. The yellow, red and the blue curves shows the current bound from PIENU [26], NA62 [9] and FASER ν [1], respectively. The black curve corresponds to DUNE ND data assuming ten years of data taking. The blue dashed curve and the green dashed curve indicate the constraints from FASER2 ν corresponding to the assumed data of one hundred times and one thousand times larger than FASER ν , respectively. We have assumed detection efficiency of 80% for FASER ν . The black dashed line shows the current constraint from Z decay [28]. The red dashed curve shows the BBN constraint [27].

stringent bound on $g_{\mu\tau}$. Finally we showed that for $g_{e\mu}$, FASER2 ν with 1000 times larger data can just slightly improve the limits (Fig. 5) for $m_{Z'} < 2$ keV and 3 MeV $< m_{Z'} < 300$ MeV.

Acknowledgments

We are very thankful to the anonymous referees, for the very useful comments and remarks. We are grateful to Y. Farzan for the useful discussion. This project has received funding from the European Union’s Horizon 2020 research and innovation programme under the Marie Skłodowska-Curie grant agreement No. 674896 and No. 690575. P.B and M.R are grateful to the IFT, UAM University for warm and generous hospitality. P.B. thanks Iran Science Elites Federation Grant No. 11131. P.B. and M.R. would like to thank the National Research Foundation of Korea Grant (NRF-2020R1I1A3072747).

[1] A. Ariga *et al.* [FASER], [arXiv:1811.10243 [physics.ins-det]].

[2] FASER Collaboration, A. Ariga *et al.*, “Technical Proposal for FASER: Forward Search Experiment at the LHC,” arXiv:1812.09139 [physics.ins-det].

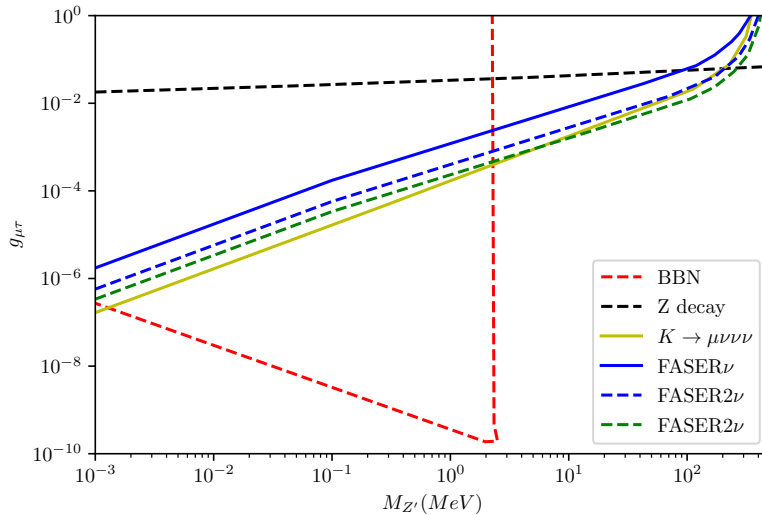


FIG. 4. The upper bound on $g_{\mu\tau}$ vs. $m_{Z'}$ at 90% C.L. The yellow and the blue curves shows the current bound from $K \rightarrow \mu\nu\nu\nu$ [20] and FASER ν , respectively. The blue dashed curve and the green dashed curve indicate the constraints from FASER2 ν corresponding to the assumed data of one hundred times and one thousand times larger than FASER ν , respectively. We have assumed detection efficiency of 80% for FASER ν . The black dashed line shows the current constraint from Z decay [28]. The red dashed curve shows the BBN constraint [27].

<http://cds.cern.ch/record/2651328>. Submitted to the CERN LHCC on 7 November 2018

- [3] H. Abreu *et al.* [FASER], *Eur. Phys. J. C* **80** (2020) no.1, 61 [arXiv:1908.02310 [hep-ex]].
- [4] X. Chu, B. Dasgupta and J. Kopp, *JCAP* **10** (2015), 011 [arXiv:1505.02795 [hep-ph]].
- [5] L. G. van den Aarssen, T. Bringmann and C. Pfrommer, *Phys. Rev. Lett.* **109** (2012), 231301 [arXiv:1205.5809 [astro-ph.CO]].
- [6] D. Hooper, M. Kaplinghat, L. E. Strigari and K. M. Zurek, *Phys. Rev. D* **76** (2007), 103515 [arXiv:0704.2558 [astro-ph]].
- [7] Y. Farzan and J. Heeck, *Phys. Rev. D* **94** (2016) no.5, 053010 [arXiv:1607.07616 [hep-ph]].
- [8] Y. Farzan and M. Tortola, *Front. in Phys.* **6** (2018) 10 [arXiv:1710.09360 [hep-ph]].
- [9] C. Lazzeroni *et al.* [NA62 Collaboration], *Phys. Lett. B* **719** (2013) 326 [arXiv:1212.4012 [hep-ex]].
- [10] P. Bakhti and Y. Farzan, *Phys. Rev. D* **95** (2017) no.9, 095008 [arXiv:1702.04187 [hep-ph]].
- [11] R. Acciarri *et al.* [DUNE Collaboration], arXiv:1512.06148 [physics.ins-det].
- [12] P. Bakhti, Y. Farzan and M. Rajaei, *Phys. Rev. D* **99** (2019) no.5, 055019 [arXiv:1810.04441 [hep-ph]].
- [13] F. Kling, *Phys. Rev. D* **102** (2020) no.1, 015007 [arXiv:2005.03594 [hep-ph]].
- [14] Y. Farzan and J. Heeck, *Phys. Rev. D* **94** (2016) no.5, 053010 [arXiv:1607.07616 [hep-ph]].
- [15] E. Fernandez-Martinez, J. Hernandez-Garcia and J. Lopez-Pavon, *JHEP* **08** (2016), 033 [arXiv:1605.08774 [hep-ph]].

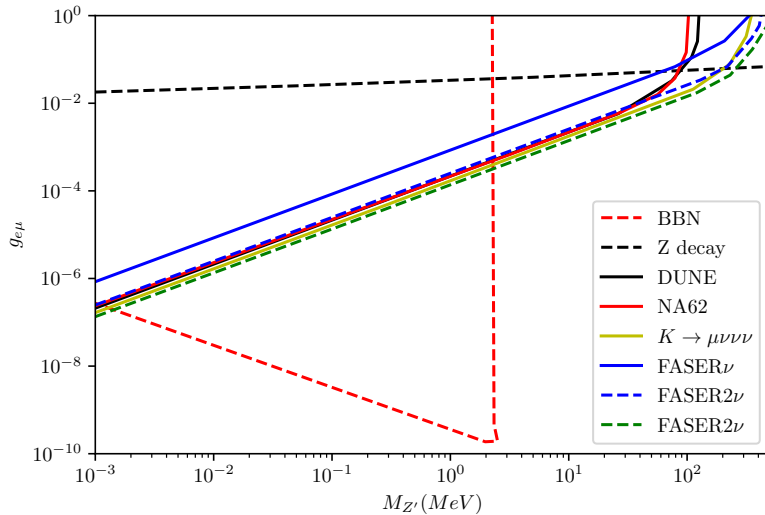


FIG. 5. The upper bound on $g_{e\mu}$ vs. $m_{Z'}$ at 90% C.L. The yellow, red and the blue curves shows the current bound from $K \rightarrow \mu\nu\nu\nu$ [20], NA62[9] and FASER ν , respectively. The black curve corresponds to DUNE ND data assuming ten years of data taking. The blue dashed curve and the green dashed curve indicate the constraints from FASER2 ν corresponding to the assumed data of one hundred times and one thousand times larger than FASER ν , respectively. We have assumed detection efficiency of 80% for FASER ν . The black dashed line shows the current constraint from Z decay [28]. The red dashed curve shows the BBN constraint [27].

- [16] R. D. Ball *et al.* [NNPDF Collaboration], *Eur. Phys. J. C* **77** (2017) no.10, 663
- [17] G. Amelino-Camelia, F. Archilli, D. Babusci, D. Badoni, G. Bencivenni, J. Bernabeu, R. A. Bertlmann, D. R. Boito, C. Bini and C. Bloise, *et al.* *Eur. Phys. J. C* **68** (2010), 619-681 [arXiv:1003.3868 [hep-ex]].
- [18] J. R. Batley *et al.* [NA48/2], *Eur. Phys. J. C* **52** (2007), 875-891 [arXiv:0707.0697 [hep-ex]].
- [19] J. Heintze, G. Heinzelmann, P. Igo-Kemenes, R. Mundhenke, H. Rieseberg, B. Schurlein, H. W. Siebert, V. Soergel, H. Stelzer and K. P. Streit, *et al.* *Nucl. Phys. B* **149** (1979), 365-380
- [20] A. V. Artamonov *et al.* [E949], *Phys. Rev. D* **94** (2016) no.3, 032012 [arXiv:1606.09054 [hep-ex]].
- [21] M. Zamkovský,
- [22] G. y. Huang, T. Ohlsson and S. Zhou, *Phys. Rev. D* **97** (2018) no.7, 075009 [arXiv:1712.04792 [hep-ph]].
- [23] R. Laha, B. Dasgupta and J. F. Beacom, *Phys. Rev. D* **89**, 093025 (2014) [arXiv:1304.3460].
- [24] M. Bordag, U. Mohideen and V. M. Mostepanenko, *Phys. Rept.* **353** (2001) 1 [quant-ph/0106045].
- [25] V. Kozhuharov [NA62], *Int. J. Mod. Phys. Conf. Ser.* **35** (2014), 1460436 [arXiv:1412.0243 [hep-ex]].

- [26] A. Aguilar-Arevalo *et al.* [PiENU], Phys. Rev. Lett. **115** (2015) no.7, 071801 [arXiv:1506.05845 [hep-ex]].
- [27] G. y. Huang, T. Ohlsson and S. Zhou, Phys. Rev. D **97** (2018) no.7, 075009 [arXiv:1712.04792 [hep-ph]].
- [28] R. Laha, B. Dasgupta and J. F. Beacom, Phys. Rev. D **89** (2014) no.9, 093025 [arXiv:1304.3460 [hep-ph]].
- [29] H. Abreu *et al.* [FASER], [arXiv:2001.03073 [physics.ins-det]].